ARMY RESEARCH LABORATORY

Light-Scattering Multipole Solution for a Cell

by Gorden Videen and Dat Ngo

ARL-TR-1725

September 1998

The findings in this report are not to be construed as an official Department of the Army position unless so designated by other authorized documents.

Citation of manufacturer's or trade names does not constitute an official endorsement or approval of the use thereof.

Destroy this report when it is no longer needed. Do not return it to the originator.

Army Research Laboratory
Adelphi, MD 20783-1197

ARL-TR-1725 **September 1998**

Light-Scattering Multipole Solution for a Cell

Gorden Videen
Information Science and Technology Directorate, ARL

Dat Ngo
NgoCo, Philadephia, PA

Abstract

We derive a multipole scattering solution for a system resembling a simple cell. In the model, a spherical cytoplasm is surrounded by a concentric cell membrane. Contained within the cytoplasm is a nonconcentric spherical nucleus. Because of the nature of the (multipole expansion) solution, numerical results can be acquired quite rapidly. We show that the resulting scatter is very sensitive to the system geometry and optical properties. Such a solution may also be used to calculate the scatter from fluorescing molecules within the cell.

Contents

Figures

1. Introduction

Light scattering is a sensitive tool that can be used to determine the geometry and composition of particle systems. This valuable tool has been used in the laboratory to characterize biological systems from bacteria to red blood cells [1–11]. The polarization state of the scattered light expressed by the light-scattering Mueller matrix has been shown to be especially sensitive to small changes in the system [5–8].

Modeling the scattering from complex cellular systems is difficult owing to their complex cellular structure, and as a result very few programs have been developed in this field. One approach has been to take advantage of the cell's relatively small refractive index within the host medium and to use the anomalous diffraction approximation [9,10]. Another approach has been to apply the finite-difference time-domain technique to cells [12,13]. Although these techniques have proven valuable, both are limited. The anomalous diffraction approximation does not accurately predict the backscatter from systems. It is in the backscatter that polarization techniques have been shown to be especially sensitive to small changes in the system geometry and chemistry. Although the finite-difference time-domain technique can model virtually any system, it is extremely computer intensive.

In this report we develop a model that can be used to approximate the scatter from a cellular system. This technique uses a multipole expansion of the fields internal and external to the cell. The model cellular system, shown in figure 1, is composed of a spherical cytoplasm surrounded by a spherical cell membrane. Contained within the cytoplasm is a spherical nucleus, which can be placed at any location within the cytoplasm. Although this model is also severely limited (since the components of the cell are restricted to being spherical), it has some advantages: calculations are very rapid and exact. This model can be used for examining the effects of various system parameters, such as the cell membrane composition or thickness, the nucleus size and position, the inclusion of organelles within the cytoplasm, or changes in the cytoplasm chemistry. The derivation of this model is similar to one given in previous works [14,15] in which we examined the scatter from a randomly placed particle within a spherical host. In the present work, a concentric outer layer is added to the host (cytoplasm) to represent a cell membrane. We show in the results section

that the inclusion of this concentric cell membrane surrounding the cytoplasm can affect the polarization state of the scattered light, especially in the backscatter region.

Finally, we note that since this is a complete solution, both the scattered and internal fields are known for the system. Using reciprocity and the solution for the internal fields, one can calculate the scattered fields from a fluorescing molecule located at any position within the cell [16].

Figure 1. Cell geometry.

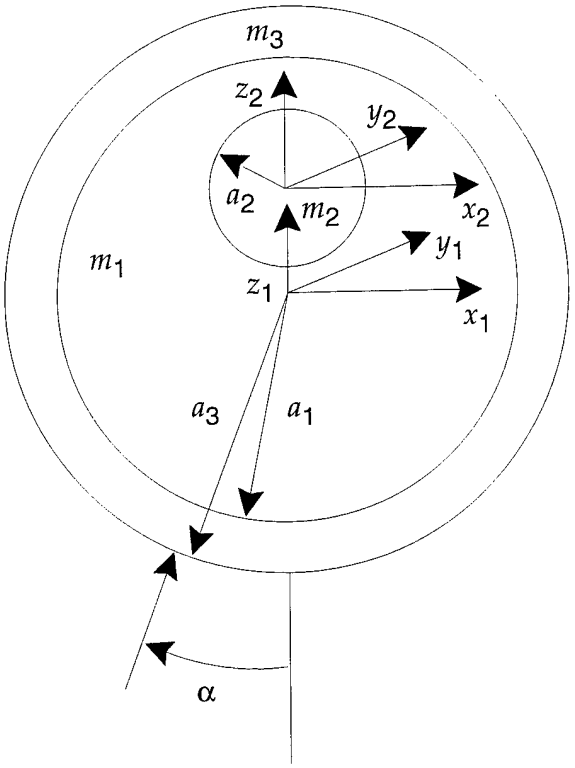

2. Solution

The geometry of the scattering system is shown in figure 1. A spherical cytoplasm of radius a_1 and complex refractive index m_1 is centered on the x_1, y_1, z_1 coordinate system. An outer, concentric cell membrane having outer radius a_3 and complex refractive index m_3 is also centered on the x_1, y_1, z_1 coordinate system such that $a_1 < a_3$. A spherical nucleus of radius a_2 and complex refractive index m_2 is centered on the x_2, y_2, z_2 coordinate system at a position $x_1 = 0$, $y_1 = 0$, $z_1 = d$ such that $a_1 - a_2 > |d|$. In order for the scattering geometry to be completely general, the wavevector of the incident radiation is oriented at angle α with respect to the z_1 axis. The wavelength and wavevector of the plane wave in the nonabsorbing, nonmagnetic incident medium are λ and k, respectively. The complex wavevector in media of refractive index m_j is k_j. To simplify the equations, we take the permeability of the spheres and the surrounding media to be the same.

We can find the scattering solution by simultaneously satisfying the boundary conditions at each interface. We consider the fields incident on each cell component separately. These fields are expanded in terms of the vector spherical harmonics, which have the following form in this derivation:

$$\begin{aligned}
\mathbf{M}^{(\rho)}_{nm,j} &= \hat{\theta}_j \left[\frac{im}{\sin\theta_j} z_n^{(\rho)}(kr_j) \tilde{P}_n^m(\cos\theta_j) e^{im\varphi_j} \right] \\
&\quad - \hat{\varphi}_j \left[z_n^{(\rho)}(kr_j) \frac{d}{d\theta_j} \tilde{P}_n^m(\cos\theta_j) e^{im\varphi_j} \right], \qquad (1) \\
\mathbf{N}^{(\rho)}_{nm,j} &= \hat{r}_j \left[\frac{1}{kr_j} z_n^{(\rho)}(kr_j) n(n+1) \tilde{P}_n^m(\cos\theta_j) e^{im\varphi_j} \right] \\
&\quad + \hat{\theta}_j \left[\frac{1}{kr_j} \frac{d}{dr_j} \left(r_j z_n^{(\rho)}(kr_j) \right) \frac{d}{d\theta_j} \tilde{P}_n^m(\cos\theta_j) e^{im\varphi_j} \right] \\
&\quad + \hat{\varphi}_j \left[\frac{1}{kr_j} \frac{d}{dr_j} \left(r_j z_n^{(\rho)}(kr_j) \right) \frac{im}{\sin\theta_j} \tilde{P}_n^m(\cos\theta_j) e^{im\varphi_j} \right], \qquad (2)
\end{aligned}$$

where the index j corresponds to the coordinate system used ($j = 1, 2$), $z_n^{(\rho)}(kr_j)$ are the spherical Bessel functions of the first, second, third, or

fourth kind ($\rho = 1, 2, 3, 4$), and

$$\tilde{P}_n^m(\cos\theta_j) = \sqrt{\frac{(2n+1)(n-m)!}{2(n+m)!}} P_n^m(\cos\theta_j), \tag{3}$$

where $P_n^m(\cos\theta_j)$ are the associated Legendre polynomials. We assume a time dependence of $\exp(-i\omega t)$.

2.1 Outer Cell-Membrane Interface

We first examine the fields that strike the outermost cell-membrane interface ($r_1 = a_3$). We consider an arbitrary field incident on the system that can be expanded with the spherical Bessel functions of the first kind, $j_n(kr_1)$:

$$\mathbf{E}_{inc}^1 = \sum_{n=0}^{\infty} \sum_{m=-n}^{n} a_{nm}\mathbf{M}_{nm,1}^{(1)} + b_{nm}\mathbf{N}_{nm,1}^{(1)}. \tag{4}$$

Similarly, the scattered electric field may be expanded with the spherical Bessel functions of the third kind, $h_n^{(1)}(kr_1)$:

$$\mathbf{E}_{sca}^1 = \sum_{n=0}^{\infty} \sum_{m=-n}^{n} c_{nm}\mathbf{M}_{nm,1}^{(3)} + d_{nm}\mathbf{N}_{nm,1}^{(3)}. \tag{5}$$

The fields inside the cell membrane may be expanded into incoming and outgoing spherical waves with spherical Bessel functions of the fourth kind, $h_n^{(2)}(k_1 r_1)$, and third kind, $h_n^{(1)}(k_1 r_1)$:

$$\mathbf{E}_{con}^1 = \sum_{n=0}^{\infty} \sum_{m=-n}^{n} i_{nm}\mathbf{M}_{nm,1}^{(3)} + j_{nm}\mathbf{N}_{nm,1}^{(3)} + k_{nm}\mathbf{M}_{nm,1}^{(4)} + l_{nm}\mathbf{N}_{nm,1}^{(4)}. \tag{6}$$

The application of boundary conditions at the outer cell-membrane interface for the above three equations yields two sets of equations:

$$a_{nm}k_3\psi_n(ka_3) + c_{nm}k_3\xi_n^{(1)}(ka_3) = i_{nm}k\xi_n^{(1)}(k_3a_3) + k_{nm}k\xi_n^{(2)}(k_3a_3), \tag{7}$$

$$a_{nm}\psi_n'(ka_3) + c_{nm}\xi_n'^{(1)}(ka_3) = i_{nm}\xi_n'^{(1)}(k_3a_3) + k_{nm}\xi_n'^{(2)}(k_3a_3), \tag{8}$$

$$b_{nm}\psi_n(ka_3) + d_{nm}\xi_n^{(1)}(ka_3) = j_{nm}\xi_n^{(1)}(k_3a_3) + l_{nm}\xi_n^{(2)}(k_3a_3), \tag{9}$$

$$b_{nm}k_3\psi_n'(ka_3) + d_{nm}k_3\xi_n'^{(1)}(ka_3) = j_{nm}k\xi_n'^{(1)}(k_3a_3) + l_{nm}k\xi_n'^{(2)}(k_3a_3), \tag{10}$$

where $\psi_n(r)$ and $\xi_n^{(q)}(r)$ $(q = 1, 2)$ are the Riccati-Bessel functions, defined by

$$\psi_n(r) = rj_n(r) \quad \text{and} \quad \xi_n^{(q)}(r) = rh_n^{(q)}(r), \tag{11}$$

and the primes denote derivatives with respect to the argument.

2.2 Cytoplasm-Cell-Membrane Interface

We now examine the fields that strike the cytoplasm-cell-membrane interface ($r_1 = a_1$). The fields in the region $|d| < r_1 < a_1$ may be expanded into incoming and outgoing spherical waves with spherical Bessel functions of the fourth kind, $h_n^{(2)}(kr_1)$, and third kind, $h_n^{(1)}(kr_1)$:

$$\mathbf{E}_{sph}^1 = \sum_{n=0}^{\infty} \sum_{m=-n}^{n} e_{nm}\mathbf{M}_{nm,1}^{(3)} + f_{nm}\mathbf{N}_{nm,1}^{(3)} + g_{nm}\mathbf{M}_{nm,1}^{(4)} + h_{nm}\mathbf{N}_{nm,1}^{(4)}. \tag{12}$$

The application of boundary conditions at the cytoplasm-cell-membrane interface yields two sets of equations:

$$i_{nm}k_1\xi_n^{(1)}(k_3a_1) + k_{nm}k_1\xi_n^{(2)}(k_3a_1) = e_{nm}k_3\xi_n^{(1)}(k_1a_1) + g_{nm}k_3\xi_n^{(2)}(k_1a_1), \tag{13}$$

$$i_{nm}\xi_n'^{(1)}(k_3a_1) + k_{nm}\xi_n'^{(2)}(k_3a_1) = e_{nm}\xi_n'^{(1)}(k_1a_1) + g_{nm}\xi_n'^{(2)}(k_1a_1), \tag{14}$$

$$j_{nm}\xi_n^{(1)}(k_3a_1) + l_{nm}\xi_n^{(2)}(k_3a_1) = f_{nm}\xi_n^{(1)}(k_1a_1) + h_{nm}\xi_n^{(2)}(k_1a_1), \tag{15}$$

$$j_{nm}k_1\xi_n'^{(1)}(k_3a_1) + l_{nm}k_1\xi_n'^{(2)}(k_3a_1) = f_{nm}k_3\xi_n'^{(1)}(k_1a_1) + h_{nm}k_3\xi_n'^{(2)}(k_1a_1). \tag{16}$$

Since our primary concern is with the scattered fields, we can write the scattered and internal field coefficients directly in terms of the cytoplasm internal field coefficients:

$$a_{nm}A_n^{(J)} + c_{nm}C_n^{(J)} = e_{nm}E_n^{(J)} + g_{nm}G_n^{(J)}, \tag{17}$$

$$b_{nm}B_n^{(J)} + d_{nm}D_n^{(J)} = f_{nm}F_n^{(J)} + h_{nm}H_n^{(J)}, \tag{18}$$

where $J = 1$ or 2. The coefficients can be found from equations (7) to (10) and (13) to (16); by applying the Wronskian formula for Riccati-Bessel functions [17]

$$W\left[\xi_n^{(1)}(z), \xi_n^{(2)}(z)\right] = -2i, \tag{19}$$

we can derive the following expressions for these coefficients:

$$A_n^{(J)} = k_1 k_3 \psi_n(ka_3)\xi_n'^{(J)}(k_3a_3) - kk_1\psi_n'(ka_3)\xi_n^{(J)}(k_3a_3), \quad (20)$$

$$B_n^{(J)} = kk_1\psi_n(ka_3)\xi_n'^{(J)}(k_3a_3) - k_1k_3\psi_n'(ka_3)\xi_n^{(J)}(k_3a_3), \quad (21)$$

$$C_n^{(J)} = k_1k_3\xi_n^{(1)}(ka_3)\xi_n'^{(J)}(k_3a_3) - kk_1\xi_n'^{(1)}(ka_3)\xi_n^{(J)}(k_3a_3), \quad (22)$$

$$D_n^{(J)} = kk_1\xi_n^{(1)}(ka_3)\xi_n'^{(J)}(k_3a_3) - k_1k_3\xi_n'^{(1)}(ka_3)\xi_n^{(J)}(k_3a_3), \quad (23)$$

$$E_n^{(J)} = kk_3\xi_n^{(1)}(k_1a_1)\xi_n'^{(J)}(k_3a_1) - kk_1\xi_n'^{(1)}(k_1a_1)\xi_n^{(J)}(k_3a_1), \quad (24)$$

$$F_n^{(J)} = kk_1\xi_n^{(1)}(k_1a_1)\xi_n'^{(J)}(k_3a_1) - kk_3\xi_n'^{(1)}(k_1a_1)\xi_n^{(J)}(k_3a_1), \quad (25)$$

$$G_n^{(J)} = kk_3\xi_n^{(2)}(k_1a_1)\xi_n'^{(J)}(k_3a_1) - kk_1\xi_n'^{(2)}(k_1a_1)\xi_n^{(J)}(k_3a_1), \quad (26)$$

$$H_n^{(J)} = kk_1\xi_n^{(2)}(k_1a_1)\xi_n'^{(J)}(k_3a_1) - kk_3\xi_n'^{(2)}(k_1a_1)\xi_n^{(J)}(k_3a_1). \quad (27)$$

2.3 Cytoplasm-Nucleus Interface

We now examine the fields that strike the cytoplasm-nucleus interface. We examine these fields in the x_2, y_2, z_2 coordinate system ($j = 2$). The fields inside the nucleus may be expressed by the spherical Bessel functions of the first kind, $j_n(k_2r_2)$:

$$\mathbf{E}_{int}^2 = \sum_{n=0}^{\infty}\sum_{m=-n}^{n} p_{nm}\mathbf{M}_{nm,2}^{(1)} + q_{nm}\mathbf{N}_{nm,2}^{(1)}. \quad (28)$$

The fields in the cytoplasm may be expressed into incoming and outgoing spherical waves by spherical Bessel functions of the fourth kind, $h_n^{(2)}(k_1r_2)$, and third kind, $h_n^{(1)}(k_1r_2)$:

$$\mathbf{E}_{ext}^2 = \sum_{n=0}^{\infty}\sum_{m=-n}^{n} r_{nm}\mathbf{M}_{nm,2}^{(3)} + s_{nm}\mathbf{N}_{nm,2}^{(3)} + t_{nm}\mathbf{M}_{nm,2}^{(4)} + u_{nm}\mathbf{N}_{nm,2}^{(4)}. \quad (29)$$

Applying boundary conditions at the inclusion sphere interface yields two sets of equations:

$$p_{nm}k_1\psi_n(k_2a_2) = r_{nm}k_2\xi_n^{(1)}(k_1a_2) + t_{nm}k_2\xi_n^{(2)}(k_1a_2), \quad (30)$$

$$p_{nm}\psi_n'(k_2a_2) = r_{nm}\xi_n'^{(1)}(k_1a_2) + t_{nm}\xi_n'^{(2)}(k_1a_2), \tag{31}$$

$$q_{nm}\psi_n(k_2a_2) = s_{nm}\xi_n^{(1)}(k_1a_2) + u_{nm}\xi_n^{(2)}(k_1a_2), \tag{32}$$

$$q_{nm}k_1\psi_n'(k_2a_2) = s_{nm}k_2\xi_n'^{(1)}(k_1a_2) + u_{nm}k_2\xi_n'^{(2)}(k_1a_2). \tag{33}$$

We can eliminate the nucleus field coefficients (p_{nm} and q_{nm}) to find relationships for the cytoplasm field coefficients. After a little bit of algebra, we have

$$r_{nm} = t_{nm}\frac{k_1\xi_n'^{(2)}(k_1a_2)\psi_n(k_2a_2) - k_2\xi_n^{(2)}(k_1a_2)\psi_n'(k_2a_2)}{k_2\xi_n^{(1)}(k_1a_2)\psi_n'(k_2a_2) - k_1\xi_n'^{(1)}(k_1a_2)\psi_n(k_2a_2)} = Q_n^r t_{nm}, \tag{34}$$

$$s_{nm} = u_{nm}\frac{k_2\xi_n'^{(2)}(k_1a_2)\psi_n(k_2a_2) - k_1\xi_n^{(2)}(k_1a_2)\psi_n'(k_2a_2)}{k_1\xi_n^{(1)}(k_1a_2)\psi_n'(k_2a_2) - k_2\xi_n'^{(1)}(k_1a_2)\psi_n(k_2a_2)} = Q_n^s u_{nm}. \tag{35}$$

The coefficients (Q_n^r and Q_n^s) are similar to the Mie scattering coefficients [18].

2.4 Fields in the Cytoplasm

The fields interior to the cytoplasm are expressed by equations (7) to (10), while the fields exterior to the nucleus are expressed by equations (34) and (35). These fields are identical. We can equate these fields and express the coefficients e_{nm}, f_{nm}, g_{nm}, and h_{nm} in terms of the coefficients r_{nm}, s_{nm}, t_{nm}, and u_{nm} using the translation addition theorem. For a translation along the z-axis with no rotation, the vector spherical harmonics are related by

$$\mathbf{M}_{nm,2}^{(q)} = \sum_{n'=0}^{\infty} A_{n'}^{(n,m)}\mathbf{M}_{n'm,1}^{(q)} + B_{n'}^{(n,m)}\mathbf{N}_{n'm,1}^{(q)}, \tag{36}$$

$$\mathbf{N}_{nm,2}^{(q)} = \sum_{n'=0}^{\infty} B_{n'}^{(n,m)}\mathbf{M}_{n'm,1}^{(q)} + A_{n'}^{(n,m)}\mathbf{N}_{n'm,1}^{(q)}, \tag{37}$$

where q denotes the order of the spherical Bessel functions ($q = 3, 4$). This relationship is valid in the region where $r > |d|$. Explicit expressions by which these coefficients can be calculated are provided in the appendix. Substituting equations (36) and (37) into equation (29) yields

$$e_{nm} = \sum_{n'=0}^{\infty} r_{n'm}A_n^{(n',m)} + s_{n'm}B_n^{(n',m)}, \tag{38}$$

$$f_{nm} = \sum_{n'=0}^{\infty} s_{n'm} A_n^{(n',m)} + r_{n'm} B_n^{(n',m)}, \tag{39}$$

$$g_{nm} = \sum_{n'=0}^{\infty} t_{n'm} A_n^{(n',m)} + u_{n'm} B_n^{(n',m)}, \quad \text{and} \tag{40}$$

$$h_{nm} = \sum_{n'=0}^{\infty} u_{n'm} A_n^{(n',m)} + t_{n'm} B_n^{(n',m)}. \tag{41}$$

Substituting equations (38) and (41) into equations (17) and (18) yields

$$a_{nm} A_n^{(J)} + c_{nm} C_n^{(J)} = \sum_{n'=0}^{\infty} t_{n'm} A_n^{(n',m)} \left[G_n^{(J)} + Q_{n'}^r E_n^{(J)} \right] + u_{n'm} B_n^{(n',m)} \left[G_n^{(J)} + Q_{n'}^s E_n^{(J)} \right] \tag{42}$$

and

$$b_{nm} B_n^{(J)} + d_{nm} D_n^{(J)} = \sum_{n'=0}^{\infty} t_{n'm} B_n^{(n',m)} \left[H_n^{(J)} + Q_{n'}^r F_n^{(J)} \right] + u_{n'm} A_n^{(n',m)} \left[H_n^{(J)} + Q_{n'}^s F_n^{(J)} \right]. \tag{43}$$

The exterior field coefficients of the nucleus, t_{nm} and u_{nm}, may be calculated if we eliminate the scattering coefficients c_{nm} and d_{nm} in equations (42) and (43):

$$a_{nm} \alpha_n = \sum_{n'=0}^{\infty} t_{n'm} T_{n'}^{(n,m,1)} + u_{n'm} U_{n'}^{(n,m,1)}, \tag{44}$$

$$b_{nm} \beta_n = \sum_{n'=0}^{\infty} t_{n'm} T_{n'}^{(n,m,2)} + u_{n'm} U_{n'}^{(n,m,2)}, \tag{45}$$

where

$$\alpha_n = A_n^{(1)} C_n^{(2)} - A_n^{(2)} C_n^{(1)}, \tag{46}$$

$$\beta_n = B_n^{(1)} D_n^{(2)} - B_n^{(2)} D_n^{(1)}, \tag{47}$$

$$T_{n'}^{(n,m,1)} = A_n^{(n',m)} \left\{ C_n^{(2)} \left[G_n^{(1)} + Q_{n'}^r E_n^{(1)} \right] - C_n^{(1)} \left[G_n^{(2)} + Q_{n'}^r E_n^{(2)} \right] \right\}, \tag{48}$$

$$T_{n'}^{(n,m,2)} = B_n^{(n',m)} \left\{ D_n^{(2)} \left[H_n^{(1)} + Q_{n'}^r F_n^{(1)} \right] - D_n^{(1)} \left[H_n^{(2)} + Q_{n'}^r F_n^{(2)} \right] \right\}, \tag{49}$$

$$U_{n'}^{(n,m,1)} = B_n^{(n',m)} \left\{ C_n^{(2)} \left[G_n^{(1)} + Q_{n'}^s E_n^{(1)} \right] - C_n^{(1)} \left[G_n^{(2)} + Q_{n'}^s E_n^{(2)} \right] \right\}, \quad (50)$$

$$U_{n'}^{(n,m,2)} = A_n^{(n',m)} \left\{ D_n^{(2)} \left[H_n^{(1)} + Q_{n'}^s F_n^{(1)} \right] - D_n^{(1)} \left[H_n^{(2)} + Q_{n'}^s F_n^{(2)} \right] \right\}. \quad (51)$$

Since the incident field coefficients are known, equations (44) and (45) represent two sets of simultaneous equations that can be solved through matrix inversion techniques for the two sets of field coefficients. Although the solution is general for any incident field, we consider specifically the case of plane-wave illumination whose wavevector is oriented at angle α with respect to the z_1 axis, as shown in figure 1. Mie scattering derivations typically restrict the plane wave so that $\alpha = 0$. Since we restrict the nucleus to be centered on the z_1 axis, we must remove the restriction on the incident plane wave for the derivation to be completely general. When the plane wave is polarized perpendicular to the x-z plane (transverse electric), the coefficients are found to be [15]

$$a_{nm} = a_{nm}^{TE} = \frac{i^n}{n(n+1)} \left[\sqrt{(n-m)(n+m+1)} \tilde{P}_n^{m+1}(\cos\alpha) - \sqrt{(n-m+1)(n+m)} \tilde{P}_n^{m-1}(\cos\alpha) \right] \quad (52)$$

$$= \frac{2i^{n+2}}{n(n+1)} \frac{\partial}{\partial\alpha} \tilde{P}_n^m(\cos\alpha), \quad (53)$$

$$b_{nm} = b_{nm}^{TE} = \frac{i^{n+2}(2n+1)}{n(n+1)} \left[\sqrt{\frac{(n-m+1)(n-m+2)}{(2n+1)(2n+3)}} \tilde{P}_{n+1}^{m-1}(\cos\alpha) + \sqrt{\frac{(n+m+1)(n+m+2)}{(2n+1)(2n+3)}} \tilde{P}_{n+1}^{m+1}(\cos\alpha) \right] \quad (54)$$

$$= \frac{2i^{n+2}}{n(n+1)} \frac{m\tilde{P}_n^m(\cos\alpha)}{\sin\alpha}. \quad (55)$$

When the plane wave is polarized in the x-z plane (transverse magnetic), the coefficients are found to be

$$a_{nm} = a_{nm}^{TM} = ib_{nm}^{TE} \quad \text{and} \quad (56)$$

$$b_{nm} = b_{nm}^{TM} = ia_{nm}^{TE}. \quad (57)$$

2.5 Scattering Amplitudes and Efficiencies

We consider the scattering amplitudes in the far field, where $kr_1 \gg ka$. The scattered fields in this case are in the $\hat{\theta}$ and $\hat{\varphi}$ directions. In this limit, the spherical Hankel functions reduce to spherical waves:

$$h_n^{(1)}(kr) \sim \frac{(-i)^n}{ikr} e^{ikr}. \tag{58}$$

The scattering amplitudes can be expressed in the form of the matrix

$$\begin{pmatrix} E\varphi^{sca} \\ E\theta^{sca} \end{pmatrix} = \frac{e^{ikr_1}}{-ikr_1} \begin{pmatrix} S_1 & S_4 \\ S_3 & S_2 \end{pmatrix} \begin{pmatrix} E_{TE}^{inc} \\ E_{TM}^{inc} \end{pmatrix}. \tag{59}$$

We solve the scattering amplitude matrix elements by expanding the scattered electric fields (eq (4)) in terms of the vector wave functions and then expanding the vector wave functions (eq (1)) in terms of the polarization directions. In the far field, the $\hat{r}$ component of the electric field becomes negligible compared with the $\hat{\theta}$ and $\hat{\varphi}$ components. After some algebra, we have the following:

$$S_1 = \sum_{n=0}^{\infty} \sum_{m=-n}^{n} (-i)^n e^{im\varphi_1} \left[d_{nm}^{TE} \frac{m}{\sin\theta_1} \tilde{P}_n^m(\cos\theta_1) + c_{nm}^{TE} \frac{\partial}{\partial\theta_1} \tilde{P}_n^m(\cos\theta_1) \right], \tag{60}$$

$$S_2 = -i \sum_{n=0}^{\infty} \sum_{m=-n}^{n} (-i)^n e^{im\varphi_1} \left[c_{nm}^{TM} \frac{m}{\sin\theta_1} \tilde{P}_n^m(\cos\theta_1) + d_{nm}^{TM} \frac{\partial}{\partial\theta_1} \tilde{P}_n^m(\cos\theta_1) \right], \tag{61}$$

$$S_3 = -i \sum_{n=0}^{\infty} \sum_{m=-n}^{n} (-i)^n e^{im\varphi_1} \left[c_{nm}^{TE} \frac{m}{\sin\theta_1} \tilde{P}_n^m(\cos\theta_1) + d_{nm}^{TE} \frac{\partial}{\partial\theta_1} \tilde{P}_n^m(\cos\theta_1) \right], \tag{62}$$

$$S_4 = \sum_{n=0}^{\infty} \sum_{m=-n}^{n} (-i)^n e^{im\varphi_1} \left[d_{nm}^{TM} \frac{m}{\sin\theta_1} \tilde{P}_n^m(\cos\theta_1) + c_{nm}^{TM} \frac{\partial}{\partial\theta_1} \tilde{P}_n^m(\cos\theta_1) \right]. \tag{63}$$

Using the following relationship for normalized, associated Legendre polynomials,

$$\tilde{P}_n^{-m}(\cos\theta_1) = (-1)^m \tilde{P}_n^m(\cos\theta_1), \tag{64}$$

we can derive the following relationships between the scattering coefficients:

$$c_{n\tilde{m}}^{TE} = (-1)^m c_{nm}^{TE},$$

$$c_{n\tilde{m}}^{TM} = (-1)^{m+1} c_{nm}^{TM},$$

$$d_{n\bar{m}}^{TE} = (-1)^{m+1} d_{nm}^{TE},$$

$$d_{n\bar{m}}^{TM} = (-1)^{m} d_{nm}^{TM}. \tag{65}$$

where $\bar{m} = -m$.

The scattering, extinction, and absorption efficiencies of the system are defined as the cross sections per projected area and may be expressed as

$$Q_{sca} = \frac{2}{(ka_1)^2}\left[\sum_{n=1}^{\infty} n(n+1) \sum_{m=-n}^{n} \left(\left|c_{nm}^{TE}\right|^2 + \left|d_{nm}^{TE}\right|^2 + \left|c_{nm}^{TM}\right|^2 + \left|d_{nm}^{TM}\right|^2\right)\right], \tag{66}$$

$$Q_{ext} = \frac{-2}{(ka_1)^2}\mathrm{Re}\left[\sum_{n=1}^{\infty} n(n+1) \sum_{m=-n}^{n} \left(c_{nm}^{TE} a_{nm}^{TE*} + d_{nm}^{TE} b_{nm}^{TE*} + c_{nm}^{TM} a_{nm}^{TM*} + d_{nm}^{TM} b_{nm}^{TM*}\right)\right], \tag{67}$$

$$Q_{abs} = Q_{ext} - Q_{sca}, \tag{68}$$

where a_{nm}^* and b_{nm}^* are the complex conjugates of a_{nm} and b_{nm}, respectively. The asymmetry parameter g is a measure of radiation pressure on the system and is a necessary parameter used in cell levitation. This quantity can be expressed as

$$\begin{aligned} g = {} & \frac{4}{Q_{sca}(ka)^2} \sum_{n,m} m\ \mathrm{Re}\left(c_{nm}^{TE} d_{nm}^{TE*} + c_{nm}^{TM} d_{nm}^{TM*}\right) \\ & + n(n+2)\sqrt{\frac{(n-m+1)(n+m+1)}{(2n+3)(2n+1)}} \\ & \times \mathrm{Re}\left[i(c_{nm}^{TE} c_{n+1m}^{TE*} + d_{nm}^{TE} d_{n+1m}^{TE*} + c_{nm}^{TM} c_{n+1m}^{TM*} + d_{nm}^{TM} d_{n+1m}^{TM*}\right]. \end{aligned} \tag{69}$$

Detailed derivations for the asymmetry parameter and the efficiencies are given elsewhere [19].

3. Results

Although equations (60) to (63) describe the electromagnetic field scattered by the cell, the meat of the problem is solving the simultaneous equations described by equations (44) and (45). For practical purposes, only a finite number N of vector spherical harmonics are necessary to describe the scatter from this system. In our calculations we use the criterion developed by Wiscombe [20] and Bohren and Huffman [18] that $N = x + 4x^{1/3} + 2$, where $x = 2\pi a_3/\lambda$. Higher order terms are insignificant, and their corresponding coefficients can safely be set to zero. We are left with solving $2N$ simultaneous equations. Solving this resulting matrix is an N^3 process, so for large size parameters the computation time slows down dramatically. For example, the CPU time required to calculate the scatter (1° scattering resolution in a plane) for an $x = 25$ cell is approximately 28 s on a SUN 4 workstation and approximately 175 s for an $x = 50$ cell.

We demonstrate one application of the model by calculating the light-scattering Mueller matrix elements for systems having slightly different parameters. Figure 2 shows these matrix elements for cells having different cell-membrane refractive indices (chemistry). The structure of the total intensity (element S_{11}) of the scattered light is essentially the same for all three systems. The positions of the maxima and minima are virtually the same, but the amplitudes of the maxima tend to increase (especially in the backscatter region) as the cell-membrane refractive index is increased. The polarization Mueller matrix elements (matrix elements S_{12}, S_{33}, and S_{34} are shown) show a marked difference. The positions of the maxima and minima remain virtually unchanged in the forward-scatter region, but in the backscatter these minima and maxima shift, and the amplitudes are significantly different. These results are consistent with previous experimental studies, which found the backscatter region of the polarization matrix elements to be extremely sensitive to small system changes [5–8]. Finally, it should be noted that the cell parameters of this figure are not realistic: the sizes are too small and the refractive indices are too large. We chose these particular parameters to illustrate the scattering effects seen. These same effects can also be seen in the scatter from cells having more realistic parameters, but because of the higher frequency oscillations in the scattering signals (oscillation

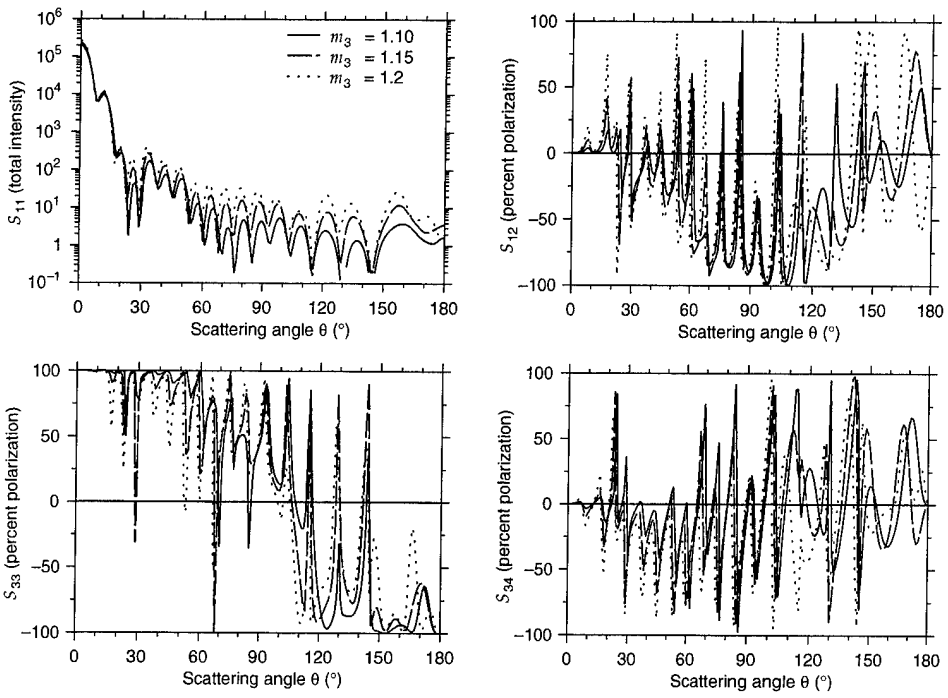

Figure 2. Light-scattering Mueller matrix elements as a function of scattering angle at three different cell-membrane refractive indices. For this system, $\lambda = 0.6328$ μm, $a_1 = 2.4$ μm, $a_2 = 1.0$ μm, $a_3 = 2.5$ μm, $m_1 = 1.05$, $m_2 = 1.15$, and $d = 1.0$ μm.

frequency increases with particle size), it is much more difficult to see any trends in the data.

Figure 3 shows the light-scattering Mueller matrix elements for cells having different nucleus positions. These results look similar to the previous results. Although the total intensity varies more than for the cell-membrane study, the polarization matrix elements still display greater sensitivity, and the backscattered light is most sensitive to changes in the system geometry.

From figures 2 and 3, it is apparent that the backscatter is the scattering region that is most sensitive to small changes in the particle geometry and chemistry. We now examine just the backscatter from a larger, more realistic cell. The system parameters are chosen to correspond to a 10-μm cell contained in an aqueous external medium ($m = 1.33$) illuminated in the near infrared ($\lambda = 850$ nm), and are similar to values used in other models [3,11,13]. Figure 4 shows the backscatter Mueller matrix for three different cytoplasm chemistries. Even though the cytoplasm refractive index change is only 1 percent between runs, the backscatter signals change significantly. The maximum oscillation frequency, which is determined primarily by the size of the cell, remains constant between runs, but the positions of the maxima and minima are shifted not only in the polarization matrix elements, but in the total intensity matrix element

S_{11} as well. Fifty-percent differences in the percent polarization signals are not uncommon.

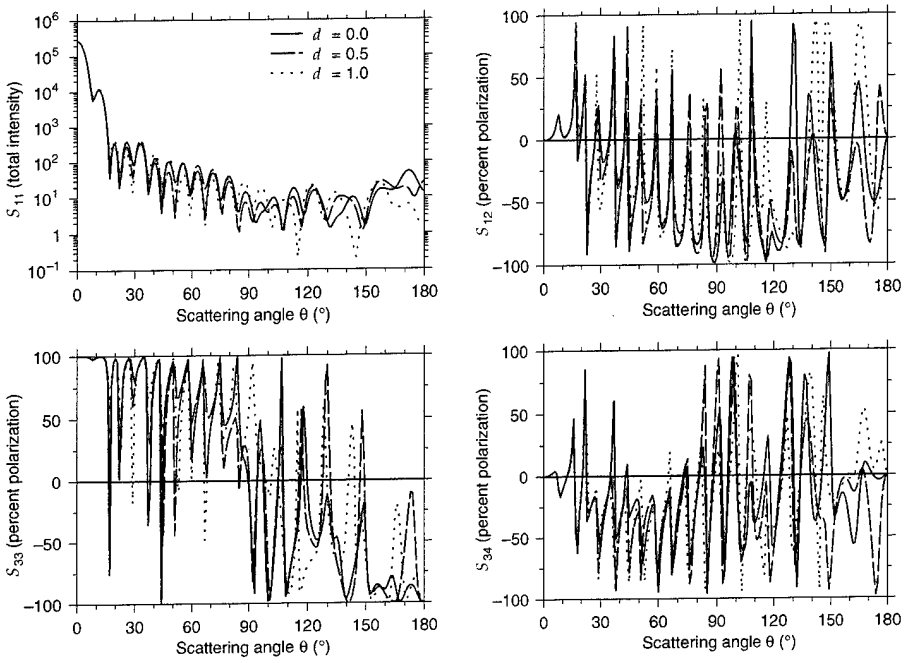

Figure 3. Light-scattering Mueller matrix elements as a function of scattering angle at three different cell nucleus locations. For this system, $\lambda = 0.6328\ \mu$m, $a_1 = 2.4\ \mu$m, $a_2 = 1.0\ \mu$m, $a_3 = 2.5\ \mu$m, $m_1 = 1.05$, $m_2 = 1.15$, and $m_3 = 1.20$.

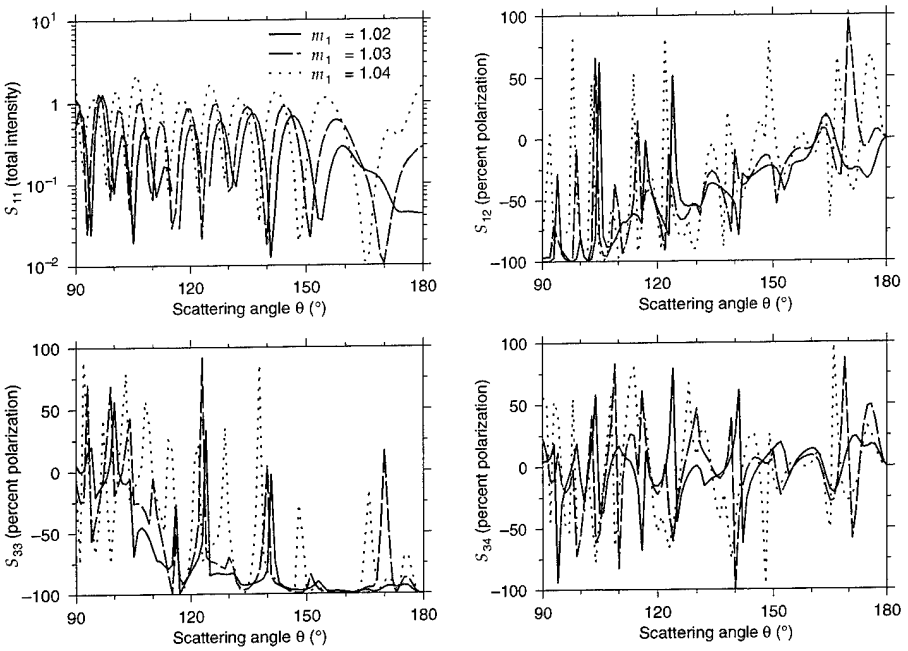

Figure 4. Light-scattering Mueller matrix elements as a function of scattering angle for three different cytoplasm chemistries. For this system, $\lambda = 0.639\ \mu$m, $a_1 = 4.99\ \mu$m, $a_2 = 2.0\ \mu$m, $a_3 = 5.0\ \mu$m, $m_2 = 1.05$, $m_3 = 1.1$, and $d = 1.0\ \mu$m.

4. Conclusion

We have derived solutions for the total field when an incident plane wave strikes a cellular system. Because of the nature of the solution, numerical results can be calculated quite rapidly compared to other techniques. The derivation places no restrictions on the refractive indices of the particle constituents or the size of the system; however, computation times increase with cell size. The model may be used for examining the sensitivity of scattering to geometrical and chemical changes of the cell. For more complicated cellular systems containing additional irregularities (such as organelles), it might be possible to calculate scattering and absorption efficiencies by incorporating effective medium approximations into the model [21,22]. The model may also be used to calculate the scatter from a fluorescing molecule located at some position within the cell. In our simulations of the light-scattering Mueller matrix, we find that the backscatter is extremely sensitive to small changes in the system parameters. We demonstrate that even a very small ($\sim$1 percent) change in system parameters can have a drastic effect on the scattered light. Since it is extremely difficult to characterize cells to such an extent, because of geometrical, orientational, and chemical changes in time, it is necessary in many modeling simulations to calculate average scattering properties, which is computationally expensive. This report provides a technique that can greatly facilitate such calculations.

Appendix. Translation Addition of Spherical Harmonics

Stein [23] and Cruzan [24] derived translation addition theorems for vector spherical wave functions. For a translation along the z-axis with no rotation, the vector spherical harmonics are related by

$$\mathbf{M}_{nm,2}^{(q)} = \sum_{n'=0}^{\infty} A_{n'}^{(n,m,q)} \mathbf{M}_{n'm,1}^{(q)} + B_{n'}^{(n,m,q)} \mathbf{N}_{n'm,1}^{(q)}, \tag{A-1}$$

$$\mathbf{N}_{nm,2}^{(q)} = \sum_{n'=0}^{\infty} B_{n'}^{(n,m,q)} \mathbf{M}_{n'm,1}^{(q)} + A_{n'}^{(n,m,q)} \mathbf{N}_{n'm,1}^{(q)}, \tag{A-2}$$

where q denotes the order of the spherical Bessel functions ($q = 3, 4$). This relationship is valid in the region where $r > |d|$. The translation coefficients $A_{n'}^{(n,m,q)}$ and $B_{n'}^{(n,m,q)}$ can be calculated from the scalar translation coefficients $C_{n'}^{(n,m,q)}$:

$$\begin{aligned} A_{n'}^{(n,m,q)} &= C_{n'}^{(n,m,q)} - \frac{k_1 d}{n'+1}\sqrt{\frac{(n'-m+1)(n'+m+1)}{(2n'+1)(2n'+3)}} C_{n'+1}^{(n,m,q)} \\ &\quad - \frac{k_1 d}{n'}\sqrt{\frac{(n'-m)(n'+m)}{(2n'+1)(2n'-1)}} C_{n'-1}^{(n,m,q)}, \end{aligned} \tag{A-3}$$

$$B_{n'}^{(n,m,q)} = \frac{-ik_1 md}{n'(n'+1)} C_{n'}^{(n,m,q)}. \tag{A-4}$$

The $C_{n'}^{(n,m,q)}$ are scalar translation coefficients. These can be found via recursion relations [19]:

$$C_{n'}^{(0,0,q)} = \sqrt{2n'+1}\, j_{n'}(k_1 d), \tag{A-5}$$

$$C_{n'}^{(-1,0,q)} = -\sqrt{2n'+1}\, j_{n'}(k_1 d), \tag{A-6}$$

$$C_{n'}^{(n+1,0,q)} = \frac{1}{(n+1)}\sqrt{\frac{2n+3}{2n'+1}}\left\{n'\sqrt{\frac{2n+1}{2n'-1}}C_{n'-1}^{(n,0,q)} + n\sqrt{\frac{2n'+1}{2n-1}}C_{n'}^{(n-1,0,q)} - (n'+1)\sqrt{\frac{2n+1}{2n'+3}}C_{n'+1}^{(n,0,q)}\right\}, \quad \text{(A-7)}$$

$$\begin{aligned}\sqrt{(n-m+1)(n+m)(2n'+1)}C_{n'}^{(n,m,q)} &= \sqrt{(n'-m+1)(n'+m)(2n'+1)}C_{n'}^{(n,m-1,q)} \\ &\quad - k_1 d\sqrt{\frac{(n'-m+2)(n'-m+1)}{(2n'+3)}}C_{n'+1}^{(n,m-1,q)} \\ &\quad - k_1 d\sqrt{\frac{(n'+m)(n'+m-1)}{(2n'-1)}}C_{n'-1}^{(n,m-1,q)}, \quad \text{(A-8)}\end{aligned}$$

and

$$C_{n'}^{(n,m,q)} = C_{n'}^{(n,-m,q)}. \quad \text{(A-9)}$$

From these equations, we see that

$$A_{n'}^{(n,m,3)} = A_{n'}^{(n,m,4)} = A_{n'}^{(n,-m,3)} = A_{n'}^{(n,m)}, \quad \text{(A-10)}$$

$$B_{n'}^{(n,m,3)} = B_{n'}^{(n,m,4)} = B_{n'}^{(n,-m,3)} = B_{n'}^{(n,m)}, \quad \text{(A-11)}$$

$$C_{n'}^{(n,m,3)} = C_{n'}^{(n,m,4)} = C_{n'}^{(n,-m,3)} = C_{n'}^{(n,m)}. \quad \text{(A-12)}$$

References

1. P. J. Wyatt, "Identification of bacteria by differential light scattering," Nature **221**, 1257–1258 (1969).

2. A. L. Koch and E. Ehrenfeld, "The size and shape of bacteria by light scattering measurements," Biochim. Biophys. Acta **165**, 262–273 (1968).

3. A. Brunsting and P. Mullaney, "Differential light scattering from spherical mammalian cells," Biophys. J. **14**, 439–453 (1974).

4. R. Meyer, "Light scattering from biological cells: Dependence of backscatter radiation on membrane thickness and refractive index," Appl. Opt. **18**, 585–588 (1979).

5. W. S. Bickel, J. F. Davidson, D. R. Huffman, and D. R. Kilkson, "Application of polarization effects in light scattering: A new biophysical tool," Proc. Nat. Acad. Sci. USA **73**, 486–490 (1976).

6. R. G. Johnston, S. B. Singham, and G. C. Salzman, "Polarized light scattering," Commun. Molec. Cell Biophys. **5**, 171–202 (1988).

7. W. P. van de Merwe, B. V. Bronk, and D. R. Huffman, "Reproducibility and sensitivity of polarized light scattering for identifying bacterial suspensions," Appl. Opt. **28**, 5052–5057 (1990).

8. B. V. Bronk, W. P. van de Merwe, and M. Stanley, "In vivo measure of average bacterial cell size from a polarized light scattering function," Cytometry **13**, 155–162 (1992).

9. G. J. Streekstra, A. G. Hoekstra, E. J. Nijhof, and R. M. Heethaar, "Light scattering by red blood cells in ektacytometry: Fraunhofer versus anomalous diffraction," Appl. Opt. **32**, 2266–2272 (1993).

10. G. J. Streekstra, A. G. Hoekstra, and R. M. Heethaar, "Anomalous diffraction by arbitrarily oriented ellipsoids: Applications in ektacytometry," Appl. Opt. **33**, 7288–7296 (1994).

11. J. Maier, S. Walker, S. Fantini, M. Franceschini, and E. Gratton, "Possible correlation between blood glucose concentration and the

reduced scattering coefficient of tissues in the near infrared," Opt. Lett. **19**, 2062–2064 (1994).

12. A. Dunn, C. Smithpeter, A. J. Welch, and R. Richards-Kortum, "Light scattering from cells," in *Biomedical Optical Spectroscopy and Diagnostics*, 1996 Technical Digest (Optical Society of America, Washington, DC, 1996), pp 50–52.

13. A. Dunn and R. Richards-Kortum, "Three-dimensional computation of light scattering from cells," IEEE J. Sel. Top. Quantum Electron. **2**, 898–905 (1996).

14. D. Ngo, G. Videen, and P. Chýlek, "A FORTRAN code for the scattering of EM waves by a sphere with a nonconcentric spherical inclusion," Comp. Phys. Commun. **1077**, 94–112 (1996).

15. G. Videen, D. Ngo, P. Chýlek, and R. G. Pinnick, "Light scattering from a sphere with an irregular inclusion," J. Opt. Soc. Am. A **12**, 922–928.

16. S. C. Hill, G. Videen, and J. D. Pendleton, "Reciprocity method for obtaining the far fields generated by a source inside or near a microparticle," J. Opt. Soc. Am. B **14**, 2522–2529 (1997).

17. M. Abramowitz and I. A. Stegun (eds.), *Handbook of Mathematical Functions* (Dover, New York, 1972).

18. C. F. Bohren and D. R. Huffman, *Absorption and Scattering of Light by Small Particles* (Wiley, New York, 1983).

19. D. Ngo, *Light Scattering from a Sphere with a Nonconcentric Spherical Inclusion*, Ph.D. dissertation, Dept. of Physics, New Mexico State University, Las Cruces (1994).

20. W. J. Wiscombe, "Improved Mie scattering algorithms," Appl. Opt. **19**, 1505–1509 (1980).

21. P. Chýlek, V. Srivastava, R. G. Pinnick, and R. T. Wang, "Scattering of electromagnetic waves by composite spherical particles: Experiment and effective medium approximations," Appl. Opt. **27**, 2396–2404 (1988).

22. G. Videen, D. Ngo, and P. Chýlek, "Effective-medium predictions of absorption by graphitic carbon in water droplets," Opt. Lett. **19**, 1675–1677 (1994).

23. S. Stein, "Addition theorems for spherical wave functions," Q. Appl. Math. **19**, 15–24 (1961).

24. O. R. Cruzan, "Translational addition theorems for spherical vector wave functions," Q. Appl. Math. **20**, 33–40 (1962).

Distribution

Admnstr
Attn Defns Techl Info Ctr
DTIC-OCP
8725 John J Kingman Rd Ste 0944
FT Belvoir VA 22060-6218

Central Intllgnc Agency
Dir DB Standard
Attn GE 47 QB
Washington DC 20505

Chairman Joint Chiefs of Staff
Attn J5 R&D Div
Washington DC 20301

Dir of Defns Rsrch & Engrg
Attn DD TWP
Attn Engrg
Washington DC 20301

Ofc of the Dir Rsrch and Engrg
Attn R Menz
Pentagon Rm 3E1089
Washington DC 20301-3080

Ofc of the Secy of Defns
Attn ODDRE (R&AT)
Attn ODDRE (R&AT) S Gontarek
The Pentagon
Washington DC 20301

OSD
Attn OUSD(A&T)/ODDDR&E(R) R J Trew
Washington DC 20301-7100

Commanding Officer
Attn NMCB23
6205 Stuart Rd Ste 101
FT Belvoir VA 22060-5275

AMCOM MRDEC
Attn AMSMI-RD W C McCorkle
Redstone Arsenal AL 35898-5240

CECOM
Attn PM GPS COL S Young
FT Monmouth NJ 07703

CECOM
Sp & Terrestrial Commctn Div
Attn AMSEL-RD-ST-MC-M H Soicher
FT Monmouth NJ 07703-5203

Dir for MANPRINT
Ofc of the Deputy Chief of Staff for Prsnnl
Attn J Hiller
The Pentagon Rm 2C733
Washington DC 20301-0300

Dir of Chem & Nuc Ops DA DCSOPS
Attn Techl Lib
Washington DC 20301

Hdqtrs Dept of the Army
Attn DAMO-FDT D Schmidt
400 Army Pentagon Rm 3C514
Washington DC 20301-0460

US Army Edgewood RDEC
Attn SCBRD-TD J Vervier
Aberdeen Proving Ground MD 21010-5423

US Army Engrg Div
Attn HNDED FD
PO Box 1500
Huntsville AL 35807

US Army Info Sys Engrg Cmnd
Attn ASQB-OTD F Jenia
FT Huachuca AZ 85613-5300

US Army Natick RDEC Acting Techl Dir
Attn SSCNC-T P Brandler
Natick MA 01760-5002

US Army NGIC
Attn Rsrch & Data Branch
220 7th Stret NE
Charlottesville VA 22901-5396

US Army Nuc & Cheml Agency
7150 Heller Loop Ste 101
Springfield VA 22150-3198

US Army Rsrch Ofc
4300 S Miami Blvd
Research Triangle Park NC 27709

US Army Simulation, Train, & Instrmntn Cmnd
Attn J Stahl
12350 Research Parkway
Orlando FL 32826-3726

Distribution (cont'd)

US Army Strtgc Defns Cmnd
Attn CSSD H MPL Techl Lib
Attn CSSD H XM Dr Davies
PO Box 1500
Huntsville AL 35807

US Army Tank-Automtv & Armaments Cmnd
Attn AMSTA-AR-TD C Spinelli
Bldg 1
Picatinny Arsenal NJ 07806-5000

US Army Tank-Automtv Cmnd Rsrch, Dev, & Engrg Ctr
Attn AMSTA-TA J Chapin
Warren MI 48397-5000

US Army Test & Eval Cmnd
Attn R G Pollard III
Aberdeen Proving Ground MD 21005-5055

US Army Train & Doctrine Cmnd
Battle Lab Integration & Techl Dirctrt
Attn ATCD-B J A Klevecz
FT Monroe VA 23651-5850

US Military Academy
Dept of Mathematical Sci
Attn MAJ D Engen
West Point NY 10996

Dept of the Navy
Chief of Nav OPS
Attn OP 03EG
Washington DC 20350

Nav Surface Warfare Ctr
Attn Code B07 J Pennella
17320 Dahlgren Rd Bldg 1470 Rm 1101
Dahlgren VA 22448-5100

GPS Joint Prog Ofc Dir
Attn COL J Clay
2435 Vela Way Ste 1613
Los Angeles AFB CA 90245-5500

DARPA
Attn B Kaspar
Attn Techl Lib
3701 N Fairfax Dr
Arlington VA 22203-1714

US Dept of Energy
Attn KK 22 K Sisson
Attn Techl Lib
Washington DC 20585

University of Texas ARL Electromag Group
Attn Campus Mail Code F0250 A Tucker
Austin TX 78713-8029

Hicks & Associates, Inc
Attn G Singley III
1710 Goodrich Dr Ste 1300
McLean VA 22102

US Army Rsrch Lab
Attn SLCRO-D
PO Box 12211
Research Triangle Park NC 27709-2211

US Army Rsrch Lab
Attn AMSRL-CI-LL Techl Lib (3 copies)
Attn AMSRL-CS-AL-TA Mail & Records Mgmt
Attn AMSRL-CS-EA-TP Techl Pub (3 copies)
Attn AMSRL-IS-EE G Videen (5 copies)
Adelphi MD 20783-1197

REPORT DOCUMENTATION PAGE

Form Approved
OMB No. 0704-0188

1. AGENCY USE ONLY *(Leave blank)*	2. REPORT DATE	3. REPORT TYPE AND DATES COVERED
	September 1998	Final, 1 October 1997 to 1 June 1998

4. TITLE AND SUBTITLE

Light-Scattering Multipole Solution for a Cell

5. FUNDING NUMBERS

DA PR: B53A
PE: 61102A

6. AUTHOR(S)

Gorden Videen (ARL) and Dat Ngo (NgoCo)

7. PERFORMING ORGANIZATION NAME(S) AND ADDRESS(ES)

U.S. Army Research Laboratory
Attn: AMSRL-IS-EE (videen@atm.dal.ca)
2800 Powder Mill Road
Adelphi, MD 20783-1197

8. PERFORMING ORGANIZATION REPORT NUMBER

ARL-TR-1725

9. SPONSORING/MONITORING AGENCY NAME(S) AND ADDRESS(ES)

U.S. Army Research Laboratory
2800 Powder Mill Road
Adelphi, MD 20783-1197

10. SPONSORING/MONITORING AGENCY REPORT NUMBER

11. SUPPLEMENTARY NOTES

AMS code: 61110253A11
ARL PR: 7FEJ70

12a. DISTRIBUTION/AVAILABILITY STATEMENT

Approved for public release; distribution unlimited.

12b. DISTRIBUTION CODE

13. ABSTRACT *(Maximum 200 words)*

We derive a multipole scattering solution for a system resembling a simple cell. In the model, a spherical cytoplasm is surrounded by a concentric cell membrane. Contained within the cytoplasm is a nonconcentric spherical nucleus. Because of the nature of the (multipole expansion) solution, numerical results can be acquired quite rapidly. We show that the resulting scatter is very sensitive to the system geometry and optical properties. Such a solution may also be used to calculate the scatter from fluorescing molecules within the cell.

14. SUBJECT TERMS

biological, polarization, Mueller matrix, scatter

15. NUMBER OF PAGES

30

16. PRICE CODE

17. SECURITY CLASSIFICATION OF REPORT	18. SECURITY CLASSIFICATION OF THIS PAGE	19. SECURITY CLASSIFICATION OF ABSTRACT	20. LIMITATION OF ABSTRACT
Unclassified	Unclassified	Unclassified	UL

NSN 7540-01-280-5500

Standard Form 298 (Rev. 2-89)
Prescribed by ANSI Std. Z39-18
298-102